2011 American Control Conference
on O'Farrell Street, San Francisco, CA, USA
June 29 - July 01, 2011

Kinetic Monte Carlo Simulation of Surface Heterogeneity in Graphite Anodes for Lithium-ion Batteries: Passive Layer Formation

Ravi N. Methekar, Paul W. C. Northrop, Kejia Chen, Richard D. Braatz, *IEEE Fellow*, and Venkat R. Subramanian

***Abstract*—The properties and chemical composition of the solid-electrolyte-interface (SEI) layer have been a subject of intense research due to their importance in the safety, capacity fade, and cycle life of Li-ion secondary batteries. Kinetic Monte Carlo (KMC) simulation is applied to explore the formation of the passive SEI layer in the tangential direction of the lithium-ion intercalation in a graphite anode. The simulations are found to consistent with observations in the literature that the active surface coverage decreases with time slowly in the initial stages of the battery operation, and then decreases rapidly. The effects of operating parameters such as the exchange current density and temperature on the formation of the passive SEI layer are investigated. The active surface coverage at the end of each charging cycle was initially lower at higher temperature, but remained constant for more cycles. The temperature that optimizes the active surface in a lithium-ion battery at Cycle 1 can result in less active surface area for most of the battery life.**

I. Introduction

Rechargeable lithium-ion batteries have been extensively used in mobile communication and portable instruments due to their high volumetric and gravimetric energy density and low self-discharge rate. The lithium-ion battery is also promising for electric (plug-in and hybrid) vehicles and stationary energy storage applications, which has motivated many scientists and engineers to work towards developing lithium-ion batteries with improved performance and longer life.

The principal components of a typical lithium-ion battery are a carbonaceous anode, an organic electrolyte, and a transition metal-oxide cathode (such as $LiCoO_2$, $LiMn_2O_4$, or $LiNiO_2$). When a carbon electrode in a non-aqueous electrolyte is charged for the first time from the open-circuit potential, lithium ions are intercalated into a carbon structure. Along with Li-ion intercalation, other (electro) chemical reactions such as decomposition of the electrolyte and the formation of a surface layer occur. This surface layer is often referred as the solid-electrolyte-interface (SEI) layer. The properties and chemical composition of the SEI layer have been a subject of intense research due to its importance in the safety, capacity fade, and the life cycle of Li-ion secondary batteries.

The SEI layer is a key element of Li-ion batteries and acts as a safety feature by maintaining a protective barrier between the negative electrode and the electrolyte. The SEI layer, which forms mainly in the first cycle of charging, should be thin, porous, and stable to provide a barrier between the electrolyte and electrode while allowing the passage of lithium ions. During the life of the battery, the battery may be subjected to unwanted conditions such as overcharging, fragmenting, and short-circuiting, which leads to the formation of byproducts. These byproducts plate the pores in the SEI layer and increase its thickness, creating a passive SEI layer, which results in increasing the resistance to the intercalation/deintercalation of lithium ions and in turn results in reducing the capacity of the battery. These phenomena can increase temperature and lead to thermal runaway. The SEI layer should be highly ion-conductive to reduce overvoltage, while being mechanically stable and flexible. These objectives require a *thin* but *stable* SEI layer that will not deteriorate or substantially change its composition or morphology with time and temperature during cycling and storage. Understanding the mechanisms of formation, growth, and reduction of the passive SEI layer could be valuable if applied to design lithium-ion batteries with increased cyclability, safety, and life.

To understand the importance of capacity fade in a lithium-ion secondary battery system, significant efforts have been devoted to the development of mathematical models that describe the discharge behavior and formation of the active and passive SEI layers. The majority of these models are empirical or semi-empirical [1],[2] which strongly depend on various empirical parameters fit to experimental data with limited predictive capability. Stamps *et al.* [3] proposed a hybrid estimation algorithm for analyzing capacity fade based on the assumption that parameters in a simple diffusion model drift slowly in between cycles; the model ignored limitations in the electrolyte phase. Arora *et al.* [4] simulated capacity fade by considering the lithium deposition as a side reaction during

Manuscript received September 20, 2010. This work was supported in part by the National Science Foundation grants under CBET-0828002, CBET-0828123, and CBET-1008692, the Institute for Advanced Computing Applications and Technologies, and the International Center for Advanced Renewable Energy and Sustainability at Washington University in St. Louis (ICARES).

R.N. Methekar was at Washington University and is currently with the GE Global Research, Bangalore, India (e-mail: ravi.methekar@ge.com).

P.W.C. Northrop is with the Department of Energy, Environmental and Chemical Engineering, Washington University in St. Louis, St. Louis, MO 63130 USA (e-mail: paul.northrop@wustl.edu)

K. Chen is with the University of Illinois, Urbana, IL 61801 USA (e-mail: kchen22@uiuc.edu).

R.D. Braatz is with the Massachusetts Institute of Technology, Cambridge, MA 02139 USA (e-mail: braatz@mit.edu).

V.R. Subramanian is with the Department of Energy, Environmental and Chemical Engineering, Washington University in St. Louis, One Brookings Drive, Campus Box 1180, St. Louis, MO 63130 USA (phone: 314-935-5676; fax: 314-935-7211; email: vsubramanian@wustl.edu).

over-charge conditions and extended this modeling concept for increasing thickness of the surface film with cycling. Ramadass *et al.* [5] presented a semi-empirical model for capacity fade that included the state of charge, solid-phase diffusion coefficient, and film resistance as a function of cycle number. Capacity fade was estimated by either accounting for active material loss, by adjusting the state of charge of the limiting electrode, or rate capacity loss, using an effective diffusion coefficient [6]. Ramadass *et al.* [7] studied capacity fade for spinel-based lithium-ion batteries through incorporation of side reaction mechanisms in the lithium-ion intercalation model. Their model assumed that the loss of the active materials with continuous cycling was attributed to a continuous film formation over the surface of the negative electrode. The model indicated that, over time, the active SEI layer becomes stable while resistance increases due to formation of the passive SEI layer. Ploehn *et al.* [8] presented a first-principles model of solvent diffusion describing the growth of a passive SEI layer. The model assumes that solvent reduction produces an insoluble product that contributes to the growth of a passive SEI layer. Their results indicate that the passive SEI layer thickness increases with the square root of time. Their findings suggest that the initial formation of a 10-100 nm thick passive SEI layer can accompany a 10-20% initial capacity loss. Zhang and White [9] considered the major mechanisms for capacity fade to be the loss of lithium ions by film formation and loss of active material in the cathode.

Bhattacharya and Van der Ven [10] performed a first-principles investigation of the concentration-dependent Li-diffusion coefficient in spinel $Li_{1+x}Ti_2O_4$ using the Kinetic Monte Carlo (KMC) simulation model proposed by Bortz *et al.* [11] They concluded that the octahedral sites are activated states for Li hops between neighboring tetrahedral sites for low lithium concentration, and that the migration barrier decreased with increased lithium concentration. The authors also provided insights into the effect of crystallographic features in spinel and layered intercalation compounds on Li mobility. First-principles investigations of lithium diffusion within the layer form of Li_xCoO_2 were explored by Van der Ven and Cedar [12]. KMC simulation was used for predicting the lithium diffusion through a deviancy mechanism for low to high concentration of lithium with isolated vacancy dilution. They concluded that migration to the adjacent vacant octahedral sites is governed by a divacancy mechanism and the migration path of this mechanism passes through a tetrahedral site. They also concluded that the activation barrier associated with the divacancy hop mechanism increases with decreasing concentration of lithium. Van der Ven *et al.* [13] studied diffusion of Li in Li_xTiS_2 for various lithium-ion concentrations using a mixed-basis cluster expansion approach. They analyzed the collective transport in concentrated intercalation compounds using atomic-scale energies to parameterize the cluster expansion Hamiltonian function, which then was used in thermodynamic and kinetic (Monte Carlo) simulations. They used the Monte Carlo algorithm proposed by Bortz *et al.* [11] with 12×12×12 Li sites. The Monte Carlo simulation used 1000 passes, where each pass corresponded to as many Li hops as there are Li sites. They postulated that the migration barriers for Li hops are very sensitive to the local environment with a lower migration barrier occurring when Li hops into a divacancy as opposed to an isolated Li vacancy. Wagemaker *et al.* [14] studied the thermodynamic and structural properties of Li_xTiO_2 spinel using a cluster expansion based on pseudo-potential ground-state energy calculations in the generalized gradient approximation. Monte Carlo simulation was used to predict the configuration space and predict thermodynamic quantities. Their Monte Carlo cell contained 10,368 Li sites with 6000 Monte Carlo passes per lattice site for each chemical potential and temperature step.

The contribution of this paper, compared to published Monte Carlo simulations, is that surface heterogeneity is explicitly addressed. This enables an exploration of passive SEI layer formation and capacity fade. Many mathematical models in the literature attempt to predict capacity fade caused by growth of the passive SEI layer in one direction, along the intercalation of Li ions. These models are not able to predict growth and formation of the passive SEI layer across the surface of the electrode particles (along the surface of the interface of the electrode and electrolyte) (see Fig. 1). It is reported in literature that the formation and growth of the passive SEI layer takes place around the electrode particle while intercalating Li^+ in the electrode particles [15]. The effect of increasing the passive SEI layer thickness along the direction of the intercalation/ deintercalation will negligibly affect the performance of the battery as compared with increasing coverage across the surface of the interface. Continuum models do not account for this surface heterogeneity, which is explored in this paper using Kinetic Monte Carlo (KMC) simulation.

The objective of this paper is to apply KMC simulation to investigate the formation and growth of the passive SEI layer, especially in the area tangential to the surface of the anode during charging and discharging cycles of lithium-ion battery. The thickness of the passive SEI layer is affected by many mechanisms such as byproduct formation, thermal runaway, and stresses in the electrodes. This paper considers the side reaction mechanism for the formation of passive SEI layer. The growth of the passive SEI layer is on the order of

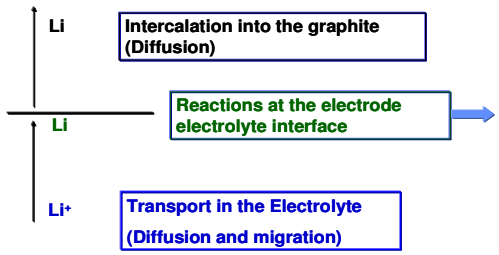

Fig. 1: Schematic representation of the multiple processes in a lithium-ion battery and the SEI layer formation at the electrode/electrolyte interface.

a few nanometers at the anode, and irreversible capacity losses due to side reactions occurs at the molecular level and are responsible for the nonidealities in the behavior of lithium-ion batteries. Hence, formation and growth of the passive SEI layer is best modeled with molecular

simulations, making KMC a more appropriate simulation method than continuum approaches.

II. Kinetic Monte Carlo (KMC) Model

In general, it is assumed that the Li-ions generated by the electrochemical reaction will move from anode to cathode or vice versa, depending on discharge or charge mode given as

$$\mathrm{CoO_2} + \mathrm{Li^+} + \mathrm{e^-} \underset{\text{Charge}}{\overset{\text{Discharge}}{\rightleftharpoons}} \mathrm{LiCoO_2} \text{ at Cathode} \qquad (1)$$

$$\mathrm{LiC_6} \underset{\text{Charge}}{\overset{\text{Discharge}}{\rightleftharpoons}} \mathrm{Li^+} + \mathrm{e^-} + \mathrm{C_6} \text{ at Anode} \qquad (2)$$

When the Li-ion reacts with the particles of the electrode in charging mode, the formation of undesired product occurs according to a side reaction such as (S = Surface)

$$\mathrm{S} + 2\mathrm{Li^+} + 2\mathrm{e^-} \rightarrow \mathrm{P} \qquad (3)$$

The undesired product (P) contributes to either increasing the thickness of the passive SEI layer or blocking the pores of the existing stable active porous SEI layer, which increases the internal resistance and decreases the rate of intercalation/deintercalation, leading to capacity fade.

KMC is used to simulate the phenomena that take place on the surface of the interface of the battery during the charging cycles. The paper considers a single electrode surface (negative electrode) and phenomena such as adsorption, desorption, surface diffusion, and formation of passive material that blocks the pores of the active SEI layer and increase the thickness of the passive SEI layer. Desorption and surface diffusion is related with stable and porous active SEI layer whereas adsorption and formation of passive materials are related with growth of the passive SEI layer. Formation and growth of the passive SEI layer is considered as a side reaction represented using the Bulter-Volmer equation. This equation considers the mechanisms of forward and backward reactions [7]. Lithium ions are intercalated on the anode surface during the charging mode of the battery. This phenomenon can be viewed as the adsorption and formation of passive materials over the electrode surface in the electrochemical reaction. Deintercalation takes place at the anode during discharging of the battery. This phenomenon can be viewed as desorption of materials from the electrode surface in the electrochemical reaction. The rate of diffusion of molecules on the surface during electrochemical reactions is modeled using a cubic lattice [15]. The intercalation of $\mathrm{Li^+}$ from electrolyte to the electrode can be described by [16]

$$\text{Adsorption rate: } K_1 C_{\mathrm{Li^+}}^{0.5} \exp(-\alpha F\eta/RT). \qquad (4)$$

The adsorbed Li can intercalate inside or diffuse on the electrode surface or form a passive layer (see Fig. 2). The liberation of Li from the electrode particle is described by [15]

$$\text{Desorption rate: } K_2 C_{\mathrm{Li^+}} \exp(\alpha F\eta/RT), \qquad (5)$$

where the nonlinear reaction rate constants K_1 and K_2 are functions of the active surface coverage, θ, and are given by:

$$K_1 = 3k_n(1-\theta)/R_{pn}, \quad K_2 = 3k_n\theta/R_{pn}. \qquad (6)$$

The value of k_n (electrochemical rate constant typically used in a continuum model) is in Table 1 and η is the overpotential given by $\eta = V - U_n$ with V being the applied voltage with respect to graphite (lower voltages results in a faster rate of charge), and the open-circuit potential U_n given by

$$U_n = 0.7222 + 0.1387\theta + 0.029\theta^{0.5} - 0.0172/\theta + 1.9\times10^{-3}/\theta^{1.5} + 0.2808\exp(0.9-15\theta) - 0.7984\exp(0.4465\theta - 0.4108) \qquad (7)$$

The surface diffusion rate is $\gamma_D\theta(1-\theta)/2$ and the passive SEI layer formation rate is $K_3\exp(-0.5F(V-0.4)/RT)$ where $K_3 = 3i_{0,P}/(R_{pn}F)$ depends on the exchange current density $i_{0,P}$ [15]. The formation of the passive SEI layer is assumed to follow Bulter-Volmer kinetics where $V - U_{n_{SEI}}$ is the overpotential for the SEI layer.

The surface KMC simulation was implemented in which the transition rates from one configuration of the lattice sites to other configurations were computed from the model in the standard way, with acceptable transitions shown in Fig. 2 [7] (see Table 1 for the list of parameters). The electrode surface was described by a 25×25 molecule mesh for a total of 625 sites (increasing the lattice size did not change the results significantly). Lithium metal formed at a site is assumed to intercalate instantaneously. The total number of lithium ions was given by the electrolyte concentration (1 M). At each KMC step, all possible transitions out of the current configuration are considered, along with their corresponding transition rates, and the new configuration r is selected that satisfies the inequality

$$\frac{\sum_{j=0}^{r-1} k_j}{\sum_{j=0}^{N} k_j} \le \chi_1 < \frac{\sum_{j=0}^{r} k_j}{\sum_{j=0}^{N} k_j} \qquad (8)$$

where k_j is the j^{th} transition rate and χ_1 is a uniformly distributed random number between zero and one. The probability of a transition selected from (8) is proportional to its transition rate. The KMC time step is calculated according to $\Delta t = -(\ln\chi_2)/\sum_{j=0}^{N} k_j$ where χ_2 is a uniformly distributed random number between zero and one and Δt is the time between transitions, typically ranging from ~10^{-9} s for the first step to 0.1 or 1 s for the final time steps [18]. The transition to the new configuration r is then executed, and the entire process is repeated. This KMC model simulates passive SEI layer formation, reduction, and growth in lithium-ion secondary batteries including in the perpendicular direction of the lithium-ion intercalation (tangential to the surface). Molecules of the same type are assumed to have an affinity for each other on the surface, with the probability of a passive molecule forming on a site being twice as high when a passive molecule is at a neighboring site. This model is similar to past KMC models for electrochemical systems [16,17]. This simulation continues until the electrode is fully charged or a time cutoff

of 1000 s was reached. The number of KMC steps in each simulation depended heavily on the cycle number and the buildup of the passive SEI layer, and ranged from several hundred to over 10,000 moves per cycle.

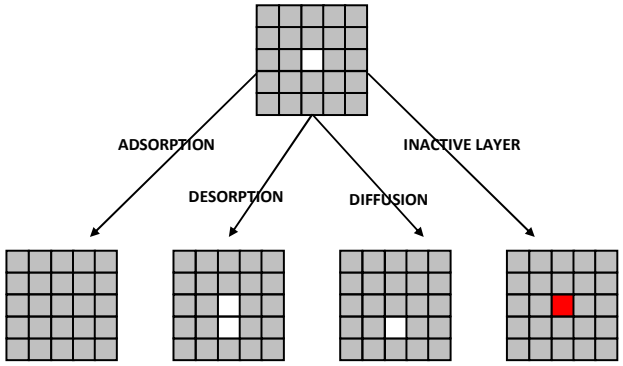

Fig. 2: Schematic representation of the phenomena represented in the KMC simulations.

The charging cycle of a lithium-ion battery is assumed under constant potential. Simulation under constant current operation is computationally more challenging [18], but can be implemented using the same KMC model [1]. All simulations in this work were implemented in Maple/MATLAB with an in-house KMC code using a personal computer with a 2.4 GHz processor and 2 GB of RAM. The results are obtained for first 100 cycles of charging. When starting each charging cycle, the surface is filled partially with active and passive atoms of the SEI layer. The surface coverage of passive atoms in the SEI layer is estimated from the previous cycle of charging and the surface coverage of active atoms is estimated using Faraday's law for discharge, which means that all the intercalated Lithium comes out during discharge. The kinetic parameters and reaction schemes are obtained from continuum models and experiments following procedures described by Drews *et al.* [19].

This type of data and analysis will help in predicting the value of the exchange current density based on the total time required for the battery to encounter failure assuming that passive layer formation is the cause of failure. The simulations were carried out at high applied potential for charging (equivalent to high currents). This paper only examines a constant potential charging protocol, rather than a constant current followed by constant potential protocol. The constant potential protocol results in a much higher charging rate during the initial seconds of any charging cycle, which tapers to zero as the battery becomes fully charged. Future work will incorporate a constant current charging protocol. Constant potential is easy to implement because the same potential is applied for main reaction and the side reaction (like two resistors in parallel). However, in a constant current charge, a fraction of the applied current would drive the main reaction, while the remainder would drive the side reaction. Furthermore, this ratio between the main and side reaction will change with time and the state of charge. Due to the high rates of charging, the time required for charging and the simulation time was reduced. Low rates of charging would make the KMC simulations computationally expensive. However, such high rates of charging enhance the rates of both intercalation and de-intercalation, which results in a high rate of byproduct formation. If the byproduct formation rate is high, then the surface coverage of the passive SEI layer IS high and capacity fade will occur at a faster rate causing the life cycle of the battery to be reduced significantly.

TABLE I
PARAMETER VALUES USED IN THE KMC SIMULATION

Symbol	Quantity	Values
a_n	specific surface area of the negative electrode, m^2/m^3	723,600
ct_n	electrolyte concentration, mol/m^3	30,555
D_{sn}	lithium-ion diffusion coefficient in the intercalation of negative electrode, m^2/s	3.9×10^{-14}
F	Faraday's constant, C/mol	96,487
i_o	exchange current density, A/m^2	1.5×10^{-9}
k_n	intercalation/deintercalation reaction rate constant, $mol/(mol/m^3)^{1.5}$	5.0307×10^{-11}
l_n	thickness of negative electrode, m	8.8×10^{-5}
R	universal gas constant, J/(mol K)	8.314
R_{pn}	radius of intercalation of negative electrode, m	2×10^{-6}
T	operating temperature, K	303.15
$U_{n,\,SEI}$	open-circuit potential of the SEI layer, V	0.4
V	applied potential, V, vs. graphite (equivalent to 4.2 – 0.001 = 4.199 V for a lithium-ion battery with the cathode operating at 4.2 V with no limitations)	0.001
α	symmetry factor for Butler-Volmer eqn.	0.5

V = volt, s = second, mol = mole, m = meter, A = ampere, J = joule, K = kelvin, C = coulomb.

III. RESULTS AND DISCUSSION

For the first charging cycle of the simulation, the active surface coverage was observed to increase with time, reaching nearly a steady-state value in ~178 s (see Fig. 3a). The rate of growth of active surface is high initially and slowly decreases. Fig. 3b shows the active surface coverage for various charging cycles. The steady-state active surface coverage is observed to decrease with increasing cycle number. The initial rate of formation of active surface is similar in each cycle, with the time to reach the steady state decreasing with increasing cycle number. The decrease in the active surface coverage is due to formation of atoms of the passive SEI layer on the same surface that is in the tangential direction to the lithium-ion intercalation.

The time required for charging decreases with the number of cycles (see Fig. 3b) due to the growth of the passive SEI layer and the reduced surface area available for the electrodeposition of active atoms and reduced capacity. Fig. 4 more clearly illustrates the dominant dynamics occurring during charging. The time scales of variation in the active surface coverage range from 0.01 to 100 s. These results suggest that the simulation time may be reduced by applying a quasi-steady-state assumption and solving the system within above mentioned time scales only, which is an

approach that has been applied in KMC simulations of other electrochemical processes [20].

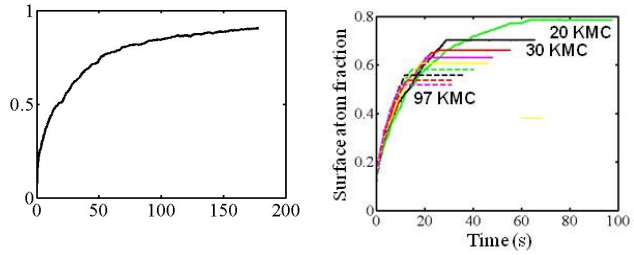

Fig. 3: (a) Time variation of the active surface coverage during the first charging cycle. (b) Time variation of the active surface coverage for 20, 30, 40, 50, 60, 70, 80, 90, 97 cycles from top to bottom (green to pink). One cycle corresponds to charging and discharge at a very low rate to avoid any current limitation (modeled using Faraday's law).

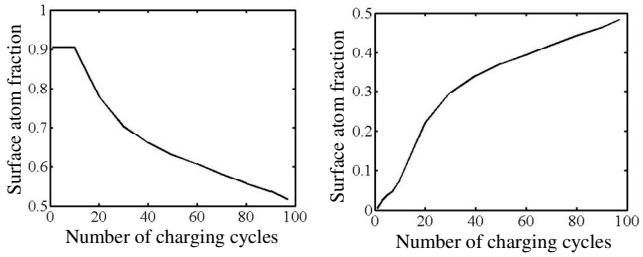

Fig. 4: (a) Time variation of the final active surface coverage at various charging cycles. (b) Time variation of the final SEI surface coverage at various charging cycles.

The active surface coverage at the end of each charging cycle is plotted with the number of charging cycles in Fig. 4a. An interesting observation is that the active surface coverage remains constant for the initial ~10 charging cycles, that is, the capacity of the lithium-ion battery does not fade for the initial cycles of charging. After this initial period, the active surface coverage decreases with cycle number and the battery capacity reduces with number of charging cycles. This behavior is consistent with observations of capacity fade in real batteries. It is generally observed experimentally that the active surface coverage decreases with time slowly in the initial stages of the battery operation, and then decreases rapidly [3]-[9]. As a battery undergoes several charging and discharging cycles, the amount of passive SEI layer on the surface becomes substantial, and less active surface area is available. This leads to a greater resistance to intercalation and deintercalation of the lithium ions and the rate of charging/ discharging drops significantly. More unwanted byproducts are formed, and active surface coverage decreases rapidly in the middle to latter stages of the battery life cycle. These experimental observations agree with the KMC simulation results in Fig. 4a.

Fig. 4b is a plot of the surface coverage of the passive SEI layer at the end of each charging cycle with number of charging cycles. The rate of formation of the passive SEI layer is initially high and reduces in latter cycles of charging. The short-time behavior of the initial charging involves the rapid formation of the first few atoms of the passive SEI layer. Though the formation of atoms of the passive SEI layer is faster initially, its concentration is not significant for making an impact on the capacity fade of the battery and we observe that the capacity of battery does not fade during first few cycles of charging. Fig. 5 shows the initial and final morphology of the surface of the anode. This shows the growth of the passive SEI layer as the battery is cycled. In the first cycle of charging, the atoms of the passive SEI layer are scattered on the surface. In the final surface structure, the passive SEI layer is formed in clusters. In this simulation, the initial surface coverage of active sites was kept at a constant value before starting the KMC simulation. Researchers have investigated the effect of various operating parameters on the formation of the passive SEI layer [3]-[9]. The effect of the exchange current density (i_0) and temperature (T) on the evolution of the active and passive surface coverages of the SEI layer are shown in Fig. 6.

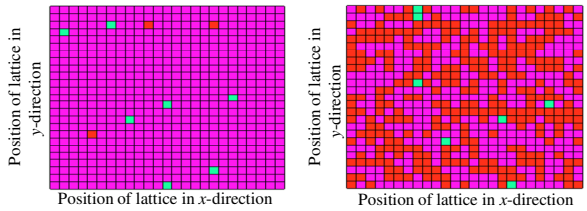

Fig. 5: (a) Initial lattice configuration of the first cycle: Magenta represents virgin sites, Red represents sites with passive SEI layer, and Green represents absorbed lithium sites. Exchange current density $i_0 = 1.5\times10^{-9}$ A/m^2. (b) Final lattice configuration of the last cycle: Magenta represents virgin sites, Red represents sites with passive SEI layer, and Green represents absorbed lithium sites. Exchange current density $i_0 = 1.5\times10^{-9}$ A/m^2.

The processes of formation of the active and passive SEI layer are a function of temperature such as in (4)-(5). The effect of temperature was investigated while keeping all other parameters at the base conditions. The active surface coverage under the fully charged condition remained constant for the lower exchange current density of 1.5×10^{-10} A/m^2 (see Fig. 6a). For an exchange current density of 1.5×10^{-9} A/m^2, the active surface coverage under fully charged conditions was initially somewhat lower for the higher temperature of 320 K, but maintained a higher value for all subsequent cycles. These results indicate that the temperature that optimizes the active surface in a lithium-ion battery at Cycle 1 can result in much lower active surface for most of the battery life. The coverage of the passive SEI layer is less at lower exchange current density and higher temperature (see Fig. 7a). It is very desirable to decrease the rate of growth of atoms of the passive SEI layer that block the pores of the stable SEI layer; on the other hand, it is not desirable to increase the temperature of the lithium-ion battery above certain values. The effect of the exchange current density on the morphology of the lattice of the electrode is observed by comparing Figs. 5 and 7a). The rate of formation of atoms of the passive SEI layer is proportional to the exchange current density, such that a decrease in the exchange current density results in a decrease in the formation of the passive SEI layer. In the base case the passive SEI layer is observed to be in the form of clusters with the longest chain containing 17 sites connected with each other (Fig. 5b) whereas with lower exchange current density the clusters are small and scattered with only 2 sites connected with each other (Fig. 7b). 48% of the lattice sites are covered for the base case compared to 6.55% for the reduced exchange current density.

Due to these high rates of charging, the electrode fails in less than 100 cycles. To make the simulations efficient, some of the important aspects like mass transfer in the electrolyte and Ohmic limitations were ignored, which are important at high rates of charging. In the future, the KMC model will be coupled with reduced order models for the continuum phases to perform multiscale simulations for a wide range of operating conditions.

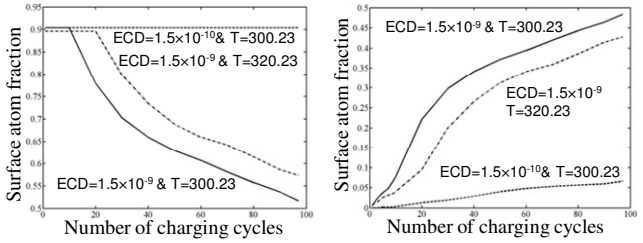

Fig. 6: Effect of ECD and temperature on the (a) depletion of active surface coverage and (b) growth of the SEI layer in a Li-ion battery (ECD = exchange current density).

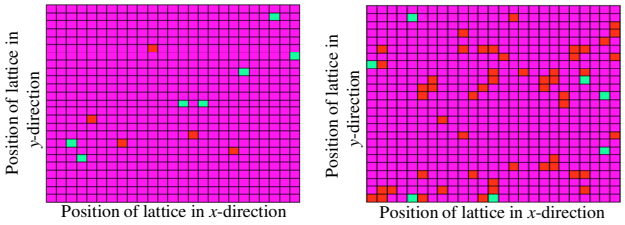

Fig. 7: (a) Initial lattice configuration of the first cycle and (b) final lattice configuration of the last cycle for ECD i_0 = 1.5×10^{-10}A/m^2. Magenta represents virgin sites, Red represents sites with passive SEI layer, and Green represents absorbed lithium sites.

IV. Conclusions

Prediction of capacity fade in lithium-ion batteries is a challenging research problem. The literature reports that the formation and growth of a passive SEI layer is mainly responsible for capacity fade in a lithium-ion secondary battery [3-6]. Passive SEI layer formation is modeled in this paper using Kinetic Monte Carlo simulation. The simulation results are in good agreement with observations reported in literature for the passive SEI layer. It was observed that the active surface coverage remains constant for the initial charging cycles and then decreases monotonically with number of charging cycles. It was also observed that the rate of formation of atoms in the passive SEI layer was high for the initial few cycles, but the amount of atoms were not significant enough to affect the capacity fade of the battery during the initial cycles of charging. The KMC simulations were able to simulate the formation of passive SEI layer atoms and subsequently the capacity fade of the lithium-ion battery. The coverage of the passive SEI layer was less at lower exchange current density, as expected. Based on the simulation parameters, higher temperature favors the main reactions (1)-(2) compared to the formation of the passive layer. This relationship may change depending on the electrolyte and chemistry. An optimal temperature may exist for minimizing the passive layer formation. In addition, the dependence of rate constants/exchange current on the temperature needs to be included to quantify the effect of temperature with reasonable confidence.

A natural next step is to dynamically couple the KMC model with continuum models for the electrolyte and solid phase, to obtain a multiscale model [19]. Such a multiscale model may enable the prediction of the formation, growth, and reduction of the passive SEI layer as well as the analysis of capacity fade. The computational cost of the continuum models can be reduced by using a reformulated model [21].

References

[1] B. Bloom, J. Cole, S. Sohn, E. Jones, V. Polzin, G. Battaglia, C. Henriksen, R. Richardson, T. Unkelhaeuser, D. Ingersoll, H.L. Case, An accelerated calendar and cycle life study of Li-ion cells. *J. Power Sources*, **101**, 238 (2001).

[2] B.Y. Liuaw, R.G. Jungst, G. Nagasubramanian, H.L. Case, D.H. Doughty, Modeling capacity fade in lithium-ion batteries. *J. Power Sources*, **140**, 157 (2005).

[3] A.T. Stamps, C.E. Holland, R.E. White, E.P. Gatzke, Analysis of capacity fade in a lithium-ion battery. *J. Power Sources*, **150**, 229 (2005).

[4] P. Arora, B.N. Popov, B. Haran, M. Ramasubramanian, S. Popova, R.E. White, Corrosion initiation time of steel reinforcement in a chloride environment—A one-dimensional solution. *Corrosion Science*, **39**, 739 (1997).

[5] P. Ramadass, A. Durairajan, B. Haran, R. White, B. Popov, Mathematical modeling of the capacity fade of Li-ion cells. *J. Electrochem. Soc.*, **149**, A54 (2002).

[6] V. Ramadesigan, V. Boovaragavan, M. Arabandi, K. Chen, H. Tuskamoto, R.D. Braatz, V.R. Subramanian, Parameter estimation and capacity fade analysis of lithium-ion batteries using first-principles-based efficient reformulated models. *ECS Trans.*, **19**, 11-19 (2009).

[7] P. Ramadass, B. Haran, R. White, B.N. Popov, Mathematical modeling of the capacity fade of Li-ion cells. *J. Power Sources*, **123**, 230 (2003).

[8] H. Ploehn, P. Ramadass, R. White, Solvent diffusion model for aging of lithium-ion battery cells. *J. Electrochem. Soc.*, **151,** A456 (2004).

[9] Q. Zhang, R. White, Capacity fade analysis of a lithium-ion cell. *J. Power Sources*, **179**, 793 (2008).

[10] J. Bhattacharya, A. Van der Ven, Phase stability and nondilute Li diffusion in spinel $Li_{1+x}Ti_2O_4$. *Phys. Rev. B*, 81, 104304 (2010).

[11] A.B. Bortz, M.H. Kalos, L. Lebowitz, Time evolution of a quenched binary alloy. II. Computer simulation of a three-dimensional model system. *J. Comput. Phys*, **17**, 10 (1975).

[12] A. Van der Ven, G. Cedar, Lithium diffusion in layered Li_xCoO_2. *Electrochem. Solid-State Lett.*, **3**, 301 (2000).

[13] A. Van der Ven, J.C. Thomas, Q. Xu, B. Swoboda, D. Morgan, Nondilute diffusion from first principles: Li diffusion in Li_xTiS_2. *Phys. Rev. B*, **78**, 104306 (2008).

[14] M. Wagemaker, A. Van der Ven, D. Morgan, G. Cedar, F.M. Mulder, G.J. Kearley, Thermodynamics of spinel Li_xTiO_2 from first principles. *Chemical Physics*, **317**, 130 (2005).

[15] G. Sikha, B. Popov, R. White, Review of models for predicting the cycling performance of lithium-ion batteries. *J. Electrochem. Soc.*, **151**, A1104 (2004).

[16] T.O. Drews, A. Radisic, J. Erlebacher, R.D. Braatz, P.C. Searson, R.C. Alkire, Stochastic simulation of the early stages of kinetically limited electrodeposition. *J. Electrochem. Soc.*, **153**, C434 (2006).

[17] T.O. Drews, R.D. Braatz, R.C. Alkire, Monte Carlo simulation of kinetically limited electrodeposition on a surface with metal seed clusters. *Z. Phys. Chem.*, **221**, 1 (2007).

[18] K. Fichthorn, W.H. Weinberg, Theoretical foundations of dynamical Monte Carlo simulations. *J. Chem. Phys.*, **95**(2), 1090 (1991).

[19] T.O. Drews, R.D. Braatz, R.C. Alkire, Coarse-grained kinetic Monte Carlo simulation of copper electrodeposition with additives. *Int. J. Multiscale Comput. Eng.*, **2**, 327 (2004).

[20] Z. Zheng, R. Stephens, R.D. Braatz, R.C. Alkire, L.R. Petzold, A hybrid multiscale kinetic Monte Carlo method for simulation of copper electrodeposition. *J. Comput. Phys.*, **227**, 5184 (2008).

[21] V. R. Subramanian, V. Boovaragavan V. Ramadesigan, M. Arabandi, Mathematical model reformulation for lithium-ion battery simulations: galvanostatic boundary conditions. *J. Electrochem. Soc.*, **156**, A260 (2009).